Water Supply

IWA PUBLISHING

Water Supply Vol 23 No 1, 144 doi: 10.2166/ws.2022.429

Development of a soil wetting pattern estimation model for drip irrigation

Yuchen Li, Wei-Bo Nie* and Zheng-Jiang Feng

State Key Laboratory of Eco-hydraulics in Northwest Arid Region, Xi'an University of Technology, Xi'an 710048, China
*Corresponding author. E-mail: nwbo2000@163.com

YL, 0000-0003-1302-512X

ABSTRACT

Accurately estimating the soil wetting pattern that closely reflects the measured value can improve the water use efficiency for drip irrigation. Ignoring the effect of the initial soil water content on the soil wetting pattern affects the accuracy of the estimated results to a certain extent. This research aimed to develop a soil wetting pattern estimation model for drip irrigation that included four easily measurable parameters (i.e., initial soil water content, saturated hydraulic conductivity, total volume of applied water, and emitter discharge rate) based on dimensional analysis theory. In this study, the wetting front advance data of 12 typical soil textures were obtained in Hydrus-2D/3D. The estimated values were then compared with measured or simulated wetting front advance values. For different experiments, the mean absolute error, root mean square error, and mean relative error varied from 2.77 to 4.69 cm, 6.20 to 10.61 cm, and 5.61% to 10.51%, respectively. Compared with the existing models, the proposed model was more consistent between the measured and simulated values. Therefore, the proposed model of this study is efficient and simple, which can help accurately estimate the soil wetting pattern of drip irrigation with a variety of soil textures.

Key words: dimensional analysis, drip irrigation, initial soil water content, point source infiltration, soil wetting pattern model

HIGHLIGHTS

- An estimation model for soil wetting patterns of drip irrigation was proposed and verified.
- Considering the initial soil water content can improve the accuracy of soil wetting pattern estimation model.
- The proposed model allows to estimate the horizontal and vertical wetting front advance and suitable for various soil textures.

GRAPHICAL ABSTRACT

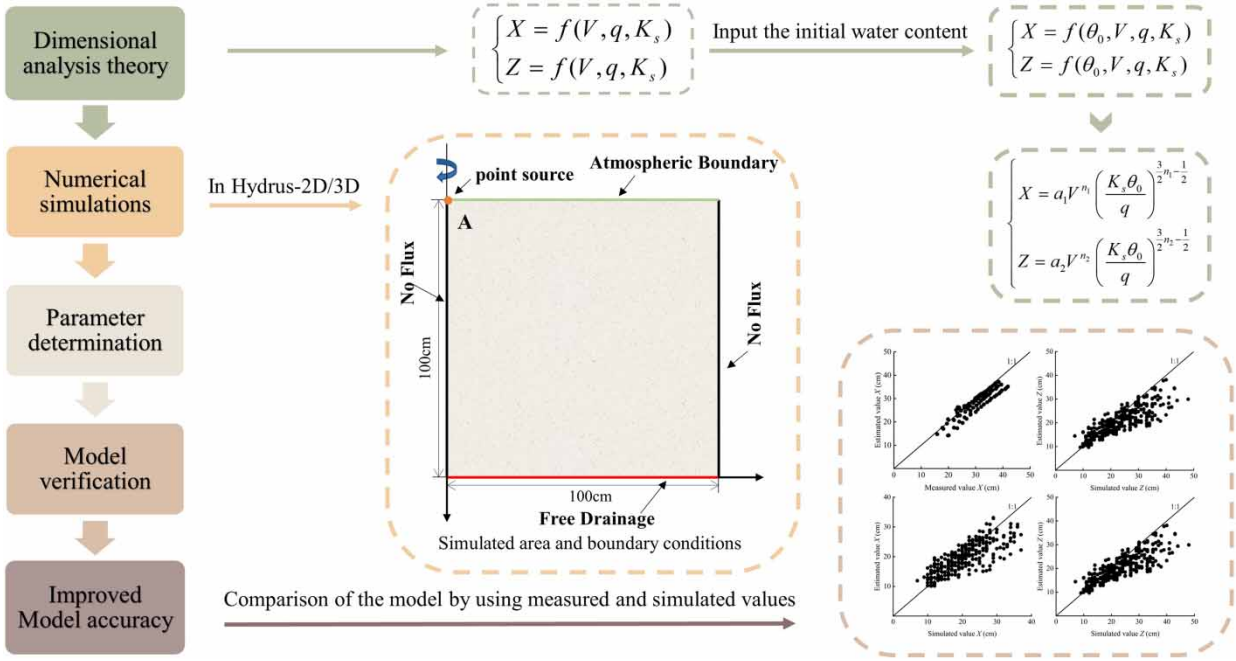

1. INTRODUCTION

Drip irrigation is one of the most common irrigation technologies, which is widely used for its high efficiency in water-saving. It helps transport water to the soil near plant roots, hence reducing water losses (from evaporation and deep drainage) and improving plant growth and water conservation (Sharmasarkar *et al.* 2001; Al-Ghobari & Dewidar 2018). The water available in the soil has a wetting pattern, the size and shape of which limit the growth of root systems and crop yields. The similarity between the soil wetting pattern and the distribution area of the crop root system is one of the critical factors used to improve irrigation performance (Wang *et al.* 2006). Access to the dimensions of the soil wetting pattern will help better determine the cover plant roots and emitter spacing, reduce the cost, and improve water use efficiency. Therefore, accurate estimation of the wetting pattern is a crucial factor in the design and management of drip irrigation systems (Subbaiah 2013). To estimate the soil wetting patterns under drip irrigation, the common models can be mainly divided into analytical models (Philip 1984; Revol *et al.* 1997; Kilic 2020), numerical models (Cote *et al.* 2003), and empirical models (Schwartzman & Zur 1986; Amin & Ekhmaj 2006; Naglič *et al.* 2014).

Analytical models have been developed on the basis of mathematical methods, physical laws, and specific assumptions (Al-Ogaidi *et al.* 2016). Moncef & Khemaies (2016) proposed an analytical method based on an assumption by Green & Ampt (1911), who assumed a piston-type flow and a semiellipsoid wetting pattern. However, according to Philip (1984), Rooij (2000), and Hill & Parlange (1972), unless the soil has a small volume, the assumption of complete water saturation in the soil profile is inconsistent with reality. Kilic (2020) developed an analytical method to describe three-dimensional (3D) wetting patterns in drip irrigation. They assumed that the composition (horizontal wetting front on the soil surface, horizontal and vertical wetting front in the soil profile) of the wetting pattern is a function of time. They further indicated that with the increase of infiltration time, the infiltration rate gradually decreases and approaches 0 cm min^{-1}, which is inconsistent with reality and does not apply to long-term irrigation. Cook *et al.* (2003) developed a user-friendly software tool called WetUp, which uses the analytical solution of Philip (1984) to estimate the wetting pattern of homogenous soils from a surface or subsurface point source and an elliptical plotting function to approximate the expected wetting patterns. However, the data used in the model as basic information from the analytical method of Philip (1984) may not be adequate to cover a wide range of soil textures and initial conditions. In addition, the tool uses the hydraulic conductivity of the wetting front as a constant value (1 mm h^{-1}), which differs from the actual field situation (Cook *et al.* 2006). Therefore, these analytical models are not widely used in the design and practice of drip irrigation systems because of their unreasonable assumptions.

Numerical models use the Richards equation as the governing equation for water flow, which mainly use the finite difference or finite element method to solve variably saturated/unsaturated flow problems (Šimůnek *et al.* 2006; Kandelous & Šimůnek 2010; Yu & Zheng 2010). Hydrus-2D/3D is the most commonly used numerical model for soil water movement processes (Skaggs *et al.* 2004; Yu & Zheng 2010). Surendran & Chandran (2022) verified that the soil water content simulated by the HYDRUS model showed agreement with observed values at different the horizontal and vertical wetting fronts from the soil profile. Hydrus-2D/3D has been used to analyze the effects of soil hydraulic properties and emitter discharge rate on the wetting pattern of drip irrigation, and it provides a reference for analyzing soil water movement with different soil textures and initial conditions (Cote *et al.* 2003; Cai *et al.* 2017; Shiri *et al.* 2020; Fan *et al.* 2021). Therefore, the simulated wetting front was obtained from the Hydrus-2D/3D model.

Empirical models are based on a regression analysis of measured or simulated values. These models help predict wetting patterns as a function of soil hydraulic properties and emitter discharge rate. Although empirical models may lack a theoretical basis, they are widely used because they are simple and closely resemble the actual situation (Karimi *et al.* 2020). The currently typical empirical models (Schwartzman & Zur 1986; Amin & Ekhmaj 2006; Naglič *et al.* 2014) are functional equations of factors that affect the wetting pattern (e.g., saturated hydraulic conductivity, total volume of applied water, and emitter discharge rate). Schwartzman & Zur (1986) developed a model for predicting the soil wetting pattern on the basis of dimensional analysis theory, including three parameters (the soil saturated hydraulic conductivity, emitter discharge rate, and total volume of applied water). However, the model lacked generality (based on the measured values of loamy and sandy soil) and did not consider the effect of the initial soil water content on the wetting front advance. Naglič *et al.* (2014) used the Hydrus-2D/3D to simulate an infiltration process with different initial conditions (11 soil textural classes, different emitter discharge rates, and varying initial soil water content), redefining the parameters of the model proposed by Schwartzman & Zur (1986) and improving the accuracy of the model. Although the initial soil water content was considered in the definition of the parameters, it was not included in the model used to estimate the wetting pattern. Amin & Ekhmaj (2006) proposed that the wetting front advance is related to the water content and added the average soil water content to the model. However, determining the average soil water content in soils with varying initial soil water content is a difficult process, and replacing half of the saturated soil water content leads to inaccurate results. In addition, these empirical models do not consider the effect of the initial soil water content on the wetting front advance or consider the average soil water content as a parameter. However, according to Witelski (2005), Subbaiah (2013), and Rooij (2000), the initial soil water content has a substantial effect on the wetting front advance. So the improved model needs to include the initial water content as a critical parameter.

Therefore, the development of an empirical model including initial soil water content that can predict the soil wetting patterns under drip irrigation would provide a convenient and accurate method to quantify the horizontal and vertical wetting front (Cristóbal-Muñoz *et al.* 2022). Moazenzadeh *et al.* (2022) believed the soil water content was helpful in determining irrigation depth and frequency, and evaluated the performance of optimization algorithms in estimating soil water content. Shiri *et al.* (2020) simulating wetting front advance in different soil types for surface and sub-surface irrigation systems through the gene expressions programming (GEP) and random forest (RF) techniques, and presented the soil water content has a higher influence on modeling vertical wetting front. Skaggs *et al.* (2010) used the Hydrus-2D/3D to simulate the effect of the initial soil water content on soil water infiltration in a drip irrigation system. The results indicated that when the initial soil water content increases in drip irrigation systems, the wetting front advance also increases, with the increase being greater in the vertical than in the horizontal direction. Jung *et al.* (2012) used X-ray photography to investigate the dynamic movement of wetting fronts and changes in the water content. The results indicated that with an increase in the initial soil water content, the wetting front changes from a bulb type to a trapezoidal type. These studies further indicated that the initial soil water content affected the wetting front advance. Meanwhile, the initial soil water content is easy to obtain experimentally, it should be regarded as a critical parameter in wetting pattern estimation models for drip irrigation.

According to previous results, the soil wetting pattern are affected by several factors including soil hydraulic properties and irrigation factors, such as soil saturated hydraulic conductivity, initial soil water content, soil textures, and emitter discharge rate (Kanda *et al.* 2020; Vishwakarma *et al.* 2022). Therefore, the objectives of this study were (1) to propose an empirical model which estimate the soil wetting pattern of drip irrigation taking the initial soil water content into account; and (2) to validate and evaluate the model proposed in this study as well as the models of Schwartzman & Zur (SZ model), Naglič *et al.* (N model), and Amin & Ekhmaj (AE model) by using laboratory experimental data and Hydrus-2D/3D simulations.

2. THEORY

2.1. Dimensional analysis

Multiple experimental and simulation studies have indicated that drip irrigation mainly exhibits a hemispherical or semielliptical soil wetting pattern (Roth 1974; Fan *et al.* 2018; Kilic 2020). The size and shape of such patterns are mainly affected by the soil hydraulic properties (e.g., soil saturated hydraulic conductivity, total volume of applied water, and initial soil water content) and irrigation factors (e.g., emitter discharge rate; Al-Ogaidi *et al.* 2016). The soil saturated hydraulic conductivity reflects the soil conditions, such as soil texture, bulk density, and pore distribution (Quirk & Schofield 1955; Buelow *et al.* 2015). Therefore, both surface ponding and runoff were ignored. According to Schwartzman & Zur (1986), these parameters can be reduced and the model can be simplified through dimensionless analysis, expressed as:

$$\begin{cases} X = f(V, q, K_s) \\ Z = f(V, q, K_s) \end{cases} \tag{1}$$

Considering the effect of the initial soil water content on the wetting front advance, the new functional relationship between these parameters can be expressed as:

$$\begin{cases} X = f(\theta_0, V, q, K_s) \\ Z = f(\theta_0, V, q, K_s) \end{cases} \tag{2}$$

where X is the horizontal wetting front advance (cm), Z is the vertical wetting front advance (cm), θ_0 is the initial soil water content ($cm^3\ cm^{-3}$), V is the total volume of applied water (L), q is the emitter discharge rate ($L\ h^{-1}$), and K_s is the soil saturated hydraulic conductivity ($cm\ h^{-1}$). Equation (2), whose specific expression requires clarification, expresses the generalized model of drip irrigation with a vertical and horizontal wetting front advance. To reduce the number of variables, Equation (2) can be simplified to three dimensionless equations. The dimensionless expressions of V^* (dimensionless total volume of applied water), X^* (dimensionless horizontal wetting front advance), and Z^* (dimensionless vertical wetting front advance) can be described as:

$$\begin{cases} V^* = V\left(\dfrac{K_s\theta_0}{q}\right)^{\dfrac{3}{2}} \\ X^* = X\left(\dfrac{K_s\theta_0}{q}\right)^{\dfrac{1}{2}} \\ Z^* = Z\left(\dfrac{K_s\theta_0}{q}\right)^{\dfrac{1}{2}} \end{cases} \tag{3}$$

These dimensionless parameters can be calculated from experimental or simulated data. Schwartzman & Zur (1986) assumed that the relationship exists between such dimensionless parameters, then:

$$\begin{cases} X^* = a_1 V^* n^1 \\ Z^* = a_2 V^* n^2 \end{cases} \tag{4}$$

where n^1 and n^2 are exponents and a_1 and a_2 are constants. Substituting Equations (3) into (4) leads to the following dimensional equation:

$$\begin{cases} X = a_1 V^{n_1}\left(\dfrac{K_s\theta_0}{q}\right)^{\dfrac{3}{2}n^1 - \dfrac{1}{2}} \\ Z = a_2 V^{n_2}\left(\dfrac{K_s\theta_0}{q}\right)^{\dfrac{3}{2}n^2 - \dfrac{1}{2}} \end{cases} \tag{5}$$

Therefore, by determining a_1, a_2, n^1, and n^2 in Equation (5), the horizontal and vertical wetting front advance can be determined under different initial conditions (V, K_s, q, and θ_0) of the drip irrigation system.

2.2. Existing models

2.2.1. SZ model

Schwartzman & Zur (1986) developed a wetting pattern estimation model (SZ model) to assess the point source infiltration of surface drip irrigation. They used the simulated and measured values of two soil textures (loamy and sandy soil) to perform a regression analysis and obtained the dimensionless power function of the total volume of applied water and horizontal and vertical wetting front advance. The model has a simple design, and the parameters required are easy to obtain through the following equations:

$$X = 1.82V^{0.22}\left(\frac{K_S}{q}\right)^{-0.17} \tag{6}$$

$$Z = 2.54V^{0.63}\left(\frac{K_S}{q}\right)^{0.45} \tag{7}$$

2.2.2. N model

Naglič *et al.* (2014) developed an improved wetting pattern estimation model (N model). To improve the accuracy of the SZ model (Schwartzman & Zur 1986), they simulated the soil water movement process of 11 soil textures (United States Department of Agriculture [USDA] soil texture classes) by using the Hydrus-2D/3D. Therefore, they obtained new parameters from 880 sets of data. The model is expressed as follows:

$$X = 1.56V^{0.29}\left(\frac{K_S}{q}\right)^{-0.06} \tag{8}$$

$$Z = 1.71V^{0.41}\left(\frac{K_S}{q}\right)^{0.11} \tag{9}$$

2.2.3. AE model

Amin & Ekhmaj (2006) introduced the average soil water content ($\Delta\theta$) into their wetting pattern estimation model (AE model). They used a nonlinear regression approach with measured values to develop their model. The model is expressed as follows:

$$X = 0.248\Delta\theta^{-0.563}V^{0.269}q^{-0.003}K_s^{-0.034} \tag{10}$$

$$Z = 2.034\Delta\theta^{-0.383}V^{0.365}q^{-0.101}K_s^{0.195} \tag{11}$$

where $\Delta\theta$ is equal to nearly half the saturated soil water content ($cm^3\ cm^{-3}$).

3. MATERIALS AND METHODS

3.1. Numerical simulations

Hydrus-2D/3D can accurately simulate the movement of soil water (Skaggs *et al.* 2010; Selim *et al.* 2013). Therefore, we used Hydrus-2D/3D to simulate the soil water infiltration process of 12 soil textures under different initial conditions. Under drip irrigation, soil water movement can be simplified as a two-dimensional (2D) movement on the axisymmetric vertical plane of a single point source centered on the emitter (Richards 1931; Cai *et al.* 2017). This process is feasible if the soil is assumed to be a homogeneous, isotropic porous medium, regardless of the effects of air resistance, temperature, and evaporation on soil

infiltration. The governing equation for water flow can be expressed as follows (Chu *et al.* 2018):

$$\frac{\partial \theta}{\partial t} = \frac{\partial}{\partial x}\left(D(\theta)\frac{\partial \theta}{\partial x}\right) + \frac{\partial}{\partial z}\left(D(\theta)\frac{\partial \theta}{\partial z}\right) - \frac{\partial K(\theta)}{\partial z}, \tag{12}$$

where x is the horizontal coordinate, z is the vertical coordinate, the positive orientation is the downward direction, θ is the soil water content ($cm^3\ cm^{-3}$), $D(\theta)$ is the unsaturated diffusion rate ($cm\ h^{-1}$), and $K(\theta)$ is the unsaturated water conductivity ($cm\ h^{-1}$). The curve representing the soil water retention characteristic, $K(\theta)$, and hydraulic conductivity is described by the soil hydraulic model. Among the common soil hydraulic models are the Brooks and Corey model (Brooks & Corey 1964) and the van Genuchten-Mualem (VG-M) model (van Genuchten 1980). The VG-M model is often used to describe soil hydraulic parameters because its parameters have clear meanings and can represent the characteristic soil water profile within the range of full negative pressure with high fitting accuracy for different types of soil (Yang *et al.* 2015). The models are expressed as follows:

$$\theta = \begin{cases} \theta_r + \dfrac{\theta_s - \theta_r}{(1 + |\alpha h|^n)^m} & (h < 0) \\ \theta_s & (h \geq 0) \end{cases} \tag{13}$$

$$K(\theta) = K_s S_e^l [1 - (1 - S_e^{l/m})^m]^2 \tag{14}$$

$$S_e = \frac{\theta - \theta_r}{\theta_s - \theta} \tag{15}$$

where θ_r is the residual soil water content ($cm^3\ cm^{-3}$), θ_s is the saturated soil water content ($cm^3\ cm^{-3}$), S_e is the relative saturation, α is an empirical parameter (cm^{-1}) inversely related to the air entry value, m and n are empirical constants ($m = 1 - 1/n$), and l is an empirical shape parameter (usually with a value of 0.5).

Infiltration space can be described as a 2D axisymmetric domain. Figure 1 shows the initial and boundary conditions. To analyze the various characteristics of wetting front advances, the horizontal distance is used to refer to the emitter spacing in the drip irrigation design without water exchange. Vertical distance is the depth from the surface of the soil to the root of the

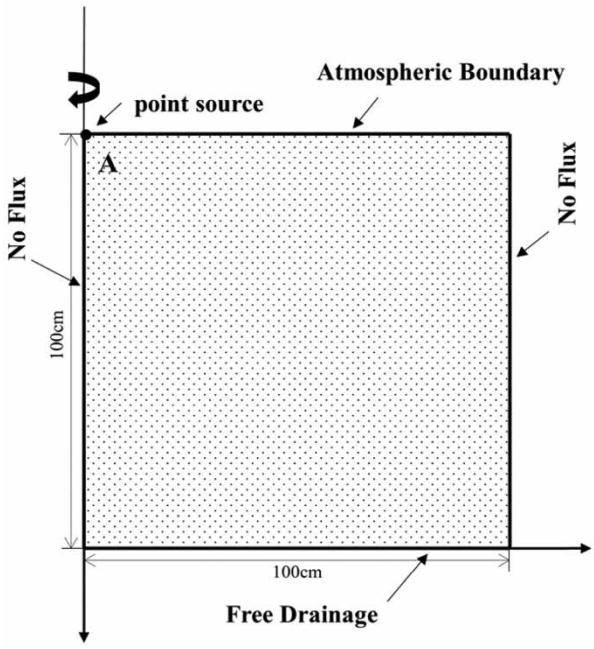

Figure 1 | Simulated area and boundary conditions.

crop and is not affected by irrigation. Therefore, the simulation area was set to a rectangular plane measuring 100 cm × 100 cm. As shown in Figure 1, point A was taken as the position of emitter discharge. The initial condition was taken as the initial soil water content, the upper boundary was taken as the atmospheric condition, and the lower boundary was taken as the free drainage condition. Both vertical boundaries were considered 'no flux' conditions. As in the study of Skaggs *et al.* (2004), the simulation time was set to 10 h, the minimum time step was 0.01 h, and the maximum time step was 0.02 h. The simulation regions in Hydrus-2D/3D were discretized into triangular meshes through finite element analysis. To increase the accuracy of the results, the maximum diameter of the outer circle of the finite element triangle was set to 1 cm (15,600 nodes in total) to refine the mesh.

Generally, the root zone soil water content should be maintained between the field capacity (FC) and permanent wilting point (PWP) values because irrigation water is wasted above the FC and crops wither below the PWP (Delgoda *et al.* 2016). Therefore, the initial soil water content can be expressed by changing the percentage of the maximum available water (AW) in the soil, which is the water volume between the permanent FC and PWP (Sreelash *et al.* 2017). Here, AW, FC, and PWP were derived from the study of Dai *et al.* (2013), and 12 typical soil types (USDA soil texture classes) were selected, the hydraulic parameters of which are presented in Table 1 (Carsel & Parrish 1988). In addition, the wetting pattern was simulated by Hydrus-2D/3D to determine the parameters of the dimensional model shown in Equation (5) by using a nonlinear regression approach.

As done in Naglič *et al.* (2014), 30, 50, and 70% of the maximum effective water were selected as the initial soil water content of different soil types (where 30 and 70% represent dry and wet soil conditions, respectively). Three common and universal emitter discharge rates (i.e., 1, 2, and 3 L h^{-1}) were set for nine soil textures (Moncef *et al.* 2002; Molavi *et al.* 2014), with smaller emitter discharge rates (i.e., 1, 1.5, and 2 L h^{-1}) selected for three finer textures to avoid surface runoff (Naglič *et al.* 2014; Moncef & Khemaies 2016). Table 2 presents the input variables for Hydrus-2D/3D.

3.2. Model verification

3.2.1. Laboratory experiment

Laboratory experimental data were collected from three infiltration experiments published in three papers (from published results; see details in Table 3; Moncef *et al.* 2002; Molavi *et al.* 2014; Naglič *et al.* 2014), including 8 sets of the horizontal and vertical wetting front advance data. These infiltration events occurred under various experimental conditions, including soil textures of sandy loam, loam, sand, sandy clay, clay, silty loam, and silt, emitter discharge rates of 1, 2 and 4 L h^{-1}, in the three different locations of the Tabriz suburbs (Molavi *et al.* 2014), the experiments under 2D soil tank consisted of 40.3 cm long, 30 cm high and 2.5 cm wide (Naglič *et al.* 2014), and infiltration experiments in semi-cylindrical container consisted of

Table 1 | Soil hydraulic parameters of 12 typical soil types

Soil texture	θ_r ($cm^3\ cm^{-3}$)	θ_s ($cm^3\ cm^{-3}$)	α (cm^{-1})	n	K_s ($cm\ h^{-1}$)	FC ($cm^3\ cm^{-3}$)	PWP ($cm^3\ cm^{-3}$)	AW ($cm^3\ cm^{-3}$)
Sand	0.045	0.43	0.145	2.68	29.70	0.08	0.05	0.03
Loamy sand	0.057	0.41	0.124	2.28	14.59	0.15	0.06	0.09
Sandy loam	0.065	0.41	0.075	1.89	4.42	0.21	0.09	0.12
Loam	0.078	0.43	0.036	1.56	1.04	0.32	0.12	0.15
Silt	0.034	0.46	0.016	1.37	0.25	0.28	0.08	0.2
Silty loam	0.067	0.45	0.020	1.41	0.45	0.29	0.14	0.2
Sandy clay loam	0.100	0.39	0.059	1.48	1.31	0.27	0.17	0.1
Clay loam	0.095	0.41	0.019	1.31	0.26	0.36	0.21	0.13
Silt clay loam	0.089	0.43	0.010	1.23	0.07	0.34	0.21	0.15
Sandy clay	0.100	0.38	0.027	1.23	0.12	0.31	0.23	0.08
Silty clay	0.070	0.36	0.005	1.09	0.02	0.35	0.25	0.10
Clay	0.068	0.38	0.008	1.09	0.20	0.36	0.27	0.09

Note. θ_r is the residual water content ($cm^3\ cm^{-3}$), θ_s is the saturated soil water content ($cm^3\ cm^{-3}$), α is the reciprocal of the air entry value (cm^{-1}), n is the experienced parameter, K_s is the saturated hydraulic conductivity ($cm\ h^{-1}$), FC is the field capacity ($cm^3\ cm^{-3}$), PWP is the permanent wilting point ($cm^3\ cm^{-3}$), and AW is the maximum available water ($cm^3\ cm^{-3}$).

Table 2 | Initial simulation conditions of drip irrigation infiltration with Hydrus-2D/3D

Soil texture	θ_0 ($cm^3\ cm^{-3}$)					
	$\theta_{30\%}$ ($cm^3\ cm^{-3}$)	$\theta_{50\%}$ ($cm^3\ cm^{-3}$)	$\theta_{70\%}$ ($cm^3\ cm^{-3}$)	q ($L\ h^{-1}$)		
Sand	0.059	0.065	0.071	1.0	2.0	3.0
Loamy sand	0.087	0.105	0.123	1.0	2.0	3.0
Sandy loam	0.126	0.150	0.174	1.0	2.0	3.0
Loam	0.185	0.215	0.245	1.0	2.0	3.0
Silt	0.140	0.180	0.220	1.0	2.0	3.0
Silty loam	0.180	0.220	0.260	1.0	2.0	3.0
Sandy clay loam	0.200	0.220	0.240	1.0	2.0	3.0
Clay loam	0.249	0.275	0.301	1.0	2.0	3.0
Silty clay loam	0.255	0.285	0.315	1.0	2.0	3.0
Sandy clay	0.254	0.270	0.286	1.0	1.5	2.0
Silty clay	0.280	0.300	0.320	1.0	1.5	2.0
Clay	0.297	0.315	0.333	1.0	1.5	2.0

Note. θ_0 is the initial soil water content ($cm^3\ cm^{-3}$), AW is the maximum available water ($cm^3\ cm^{-3}$), PWP is the permanent wilting point ($cm^3\ cm^{-3}$), and q is the emitter discharge rate ($L\ h^{-1}$). Here, $\theta_{30\%} = 30\%$ AW + PWP, $\theta_{50\%} = 50\%$ AW + PWP, and $\theta_{70\%} = 70\%$ AW + PWP.

120 cm high and 150 cm in diameter (Moncef *et al.* 2002). More details of the experiments can be found in Molavi *et al.* (2014), Naglič *et al.* (2014) and Moncef *et al.* (2002).

3.2.2. Simulation experiment

Simulation values were used to evaluate the SZ model, the N model, and the AE model and the proposed model to verify its reliability. The initial soil water content was selected as 40 and 60% of the AW, and the four models were verified using the soil hydraulic parameters presented in Table 1. The input variables used in Hydrus-2D/3D for validation are presented in Table 4. A total of 72 groups of experiments were conducted and included 2 initial soil water concentrations, 12 soil textures (USDA soil texture classes), and 3 emitter discharge rates (i.e., 1, 1.5/2, and 3 $L\ h^{-1}$).

3.3. Criteria for model evaluation

The performance of each model was evaluated by comparing the estimated statistics for the horizontal and vertical wetting front advance of drip irrigation with measured values (Moncef *et al.* 2002; Molavi *et al.* 2014; Naglič *et al.* 2014) or simulated values in Hydrus-2D/3D. The assessment indicators were the mean absolute error (MAE), mean relative error (MRE), and

Table 3 | Details of the laboratory experimental data sets

	Soil texture	K_s ($cm\ h^{-1}$)	q ($L\ h^{-1}$)			θ_0 ($cm^3\ cm^{-3}$)	θ_s ($cm^3\ cm^{-3}$)
Molavi *et al.* (2014)	Sandy loam	2.13	2	4		0.07	0.44
	Sandy loam	1.62	2	4		0.10	0.38
	Loam	0.78	2	4		0.14	0.38
Naglič *et al.* (2014)	Sand	29.70	2			0.06	0.44
	Sandy clay	0.12	2			0.27	0.38
	Clay	0.20	2			0.32	0.38
	Silty loam	0.45	2			0.22	0.45
Moncef *et al.* (2002)	Silt	5.80	1	2	4	0.27	0.58

Note. K_s is the saturated hydraulic conductivity ($cm\ h^{-1}$), q is the emitter discharge rate ($L\ h^{-1}$), θ_0 is the initial soil water content ($cm^3\ cm^{-3}$), and θ_s is the saturated soil water content ($cm^3\ cm^{-3}$).

Table 4 | Simulation of the initial conditions for validation with Hydrus-2D/3D

Soil texture	K_s (cm h^{-1})	q (L h^{-1})			θ_0 (cm^3 cm^{-3})	
					$\theta_{40\%}$ (cm^3 cm^{-3})	$\theta_{60\%}$ (cm^3 cm^{-3})
Sand	29.70	1	2	3	0.062	0.068
Loamy sand	14.59	1	2	3	0.096	0.114
Sandy loam	4.42	1	2	3	0.138	0.162
Loam	1.04	1	2	3	0.200	0.230
Silt	0.25	1	2	3	0.160	0.200
Silty loam	0.45	1	2	3	0.200	0.240
Sandy clay loam	1.31	1	2	3	0.210	0.230
Clay loam	0.26	1	2	3	0.262	0.288
Silty clay loam	0.07	1	2	3	0.270	0.300
Sandy clay	0.12	1	1.5	2	0.262	0.278
Silty clay	0.02	1	1.5	2	0.290	0.310
Clay	0.20	1	1.5	2	0.306	0.324

Note. K_s is the saturated hydraulic conductivity (cm h^{-1}), q is the emitter discharge rate (L h^{-1}), θ_0 is the initial soil water content (cm^3 cm^{-3}), AW is the maximum available water (cm^3 cm^{-3}), and PWP is the permanent wilting point (cm^3 cm^{-3}). Here, $\theta_{40\%} = 40\%$ AW + PWP and $\theta_{60\%} = 60\%$ AW + PWP.

root mean square error (RMSE) (Willmott *et al.* 2012), which can be calculated as follows:

$$\mathrm{MAE} = \frac{1}{N}\sum_{i=1}^{N}|y_{ei} - y_{mi}| \tag{16}$$

$$\mathrm{MRE} = \frac{1}{N}\sum_{i=1}^{N}\left(\frac{y_{ei} - y_{mi}}{y_{mi}}\right) \times 100\% \tag{17}$$

$$\mathrm{RMSE} = \sqrt{\frac{1}{N}\sum_{i=1}^{N}(y_{ei} - y_{mi})^2} \tag{18}$$

where i is an integer varying from 1 to N, N is the total number of data sets, y_{ei} is the ith estimated value, and y_{mi} is the ith measured or simulated value. Generally, the MAE, RMSE, and MRE allow for quantitative comparisons of estimated values with measured or simulated values for the horizontal and vertical wetting front advance. Lower MAE and RMSE values indicate a more favorable model fit. If MRE is less than $\pm 10\%$, then the MRE is considered to be within a highly accurate range (Chai & Draxler 2014; Nie *et al.* 2018).

4. RESULTS

4.1. Parameter determination

Regression analysis of the results obtained with Hydrus-2D/3D simulations under the conditions shown in Table 2 revealed optimal parameter values of Equation (5) for horizontal (a_1, n_1) and vertical (a_2, n_2) wetting front advances of 0.98, 0.29 and 1.89, 0.41, respectively. In addition, the relationship between the dimensionless cumulative infiltration V^*, dimensionless horizontal wetting front advance X^*, and dimensionless vertical wetting front advance Z^* demonstrated a favorable fit with coefficients of determination (R^2) of 0.937 and 0.929 (Figure 2). By substituting these parameters into Equation (5),

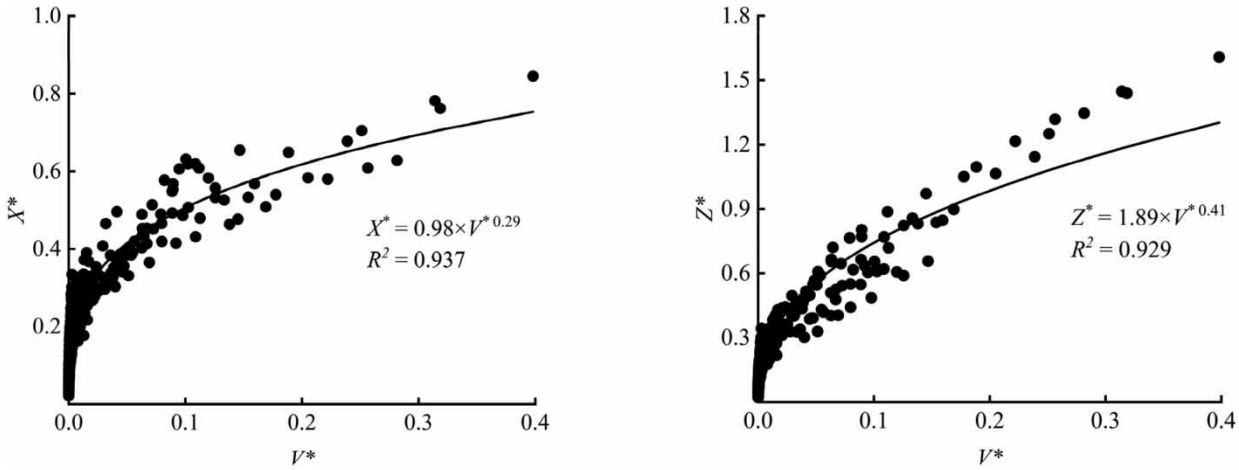

Figure 2 | Relationship between the dimensionless total volume of applied water V^* and horizontal X^* or vertical Z^* wetting front advance.

the horizontal and vertical wetting front advances could be estimated using the following equations:

$$X = 0.98V^{0.29}\left(\frac{K_S\theta_0}{q}\right)^{-0.07} \tag{19}$$

$$Z = 1.89V^{0.41}\left(\frac{K_S\theta_0}{q}\right)^{0.11} \tag{20}$$

To ensure the accuracy of Equations (19) and (20), the MAE, RMSE, and MRE of the simulated and estimated values (horizontal and vertical wetting front) were calculated. The obtained results indicated that the MAE, RMSE, and MRE ranged from 2.77 to 4.02 cm, from 3.75 to 6.32 cm, and from 6.91% to 8.46%, respectively. In addition, the high R^2 and low errors observed (Figure 2) between the estimated and simulated values indicated the high accuracy of Equations (19) and (20).

4.2. Comparison of the four models by using measured values

To verify the reliability of the SZ model, represented by Equations (6) and (7); the N model, represented by Equations (8) and (9); the AE model, represented by Equations (10) and (11); and the proposed model, represented by Equations (19) and (20), we used the values of K_s, q, θ_0, and $\Delta\theta$ (half the saturated water content value) in Table 3 to estimate the horizontal and vertical wetting front advance. We then compared these estimated values with the measured values. The results are presented in Figure 3 and Table 5.

As shown in Figure 3, the estimated values of the four models agreed with the measured values and were evenly distributed on both sides of the 1:1 line. Table 5 shows the MAE, MRE, and RMSE values calculated for analyzing the measured and estimated values. The proposed model exhibited the smallest error in the horizontal and vertical wetting front advance distance, with MAE values of 2.77 and 3.56 cm, RMSE values of 6.45 and 10.61 cm, and MRE values of 9.04% and 10.51%, respectively. Following the proposed model, the AE model and the N model demonstrated similar results, with MAE values of 2.91 and 4.99 cm and 2.91 and 5.08 cm, RMSE values of 6.59 and 11.32 cm and 7.78 and 11.34 cm, and MRE values of 9.46% and 13.75% and 10.50% and 15.84%, respectively. The SZ model exhibited the largest error, with MAE values of 4.13 and 5.19 cm, RMSE values of 7.56 and 12.90 cm, and MRE values of 14.01% and 15.78%, respectively. These results indicated that the estimated values of the four models were consistent with the measured values, although some differences were observed. These differences were mainly due to inevitable experimental errors and the simplified assumptions of the models. The SZ model has the lowest consistency of the four models since the effect of initial soil water content was not taken into account and that only two soil textures (loam and sand) were included instead of a variety of soil textures. Because the effect of soil water content was not neglected, the results of the N model and AE model are similar and more consistent than those of the SZ model. Although Naglič *et al.* (2014) considered the initial soil water content in the parameter definition, the N model did not include the initial soil water content. Amin & Ekhmaj (2006) proposed that the

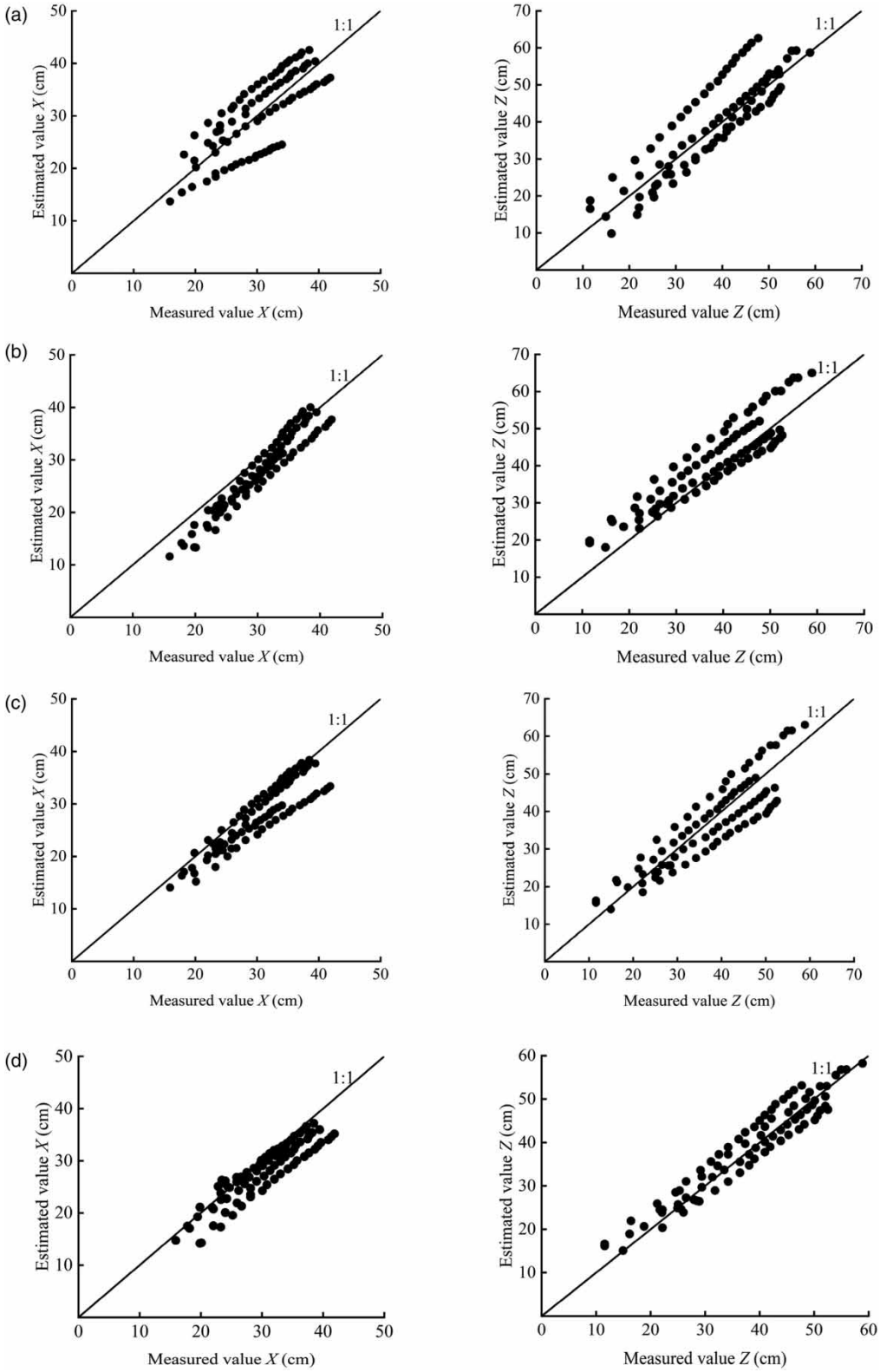

Figure 3 | Comparison of the measured and estimated values of the horizontal X and vertical Z wetting front advance. (a) SZ model. (b) N model. (c) AE model. (d) Proposed model.

Table 5 | Error analysis of the measured and estimated values of the wetting front advance

	Horizontal wetting front advance			Vertical wetting front advance		
	MAE (cm)	RMSE (cm)	MRE (%)	MAE (cm)	RMSE (cm)	MRE (%)
SZ model	4.13	7.56	14.01	5.19	12.90	15.78
N model	2.91	7.78	10.50	5.08	11.34	15.84
AE model	2.91	6.59	9.46	4.99	11.32	13.75
Proposed model	2.77	6.45	9.04	3.56	10.61	10.51

Note. MAE, mean absolute error; RMSE, root mean square error; MRE, mean relative error.

wetting front advance was affected by soil water content and added the average soil water content to the model. However, it was found that the results of the AE model for the soil wetting front with different initial soil water contents were not as accurate as the model proposed in this paper. This indicated that the initial soil water content in the AE model could not be replaced by half of the saturated soil water content.

Overall, the estimated values of the proposed model were more accurate than those of the SZ model, the N model, and the AE model. This is because the proposed model considers the effect of the initial soil water content on wetting front advance, which is more consistent with the actual infiltration process. During the infiltration process, any variations in the initial soil water content result in different advance rates of the wetting front. Soils with high initial soil water content require less water to fill soil pores, whereas soils with low initial soil water content require more water to fill soil pores. Therefore, soils with higher water content have a higher wetting front advance speed, which is why ignoring the initial soil water content leads to inaccurate results. In conclusion, this study, the proposed model based on the dimensional analytical approach with the initial soil water content considered simultaneously, exhibits improved accuracy over existing models, and obtains more consistency between estimated and measured values.

4.3. Comparison of the four models by using simulation values

First, Hydrus-2D/3D was used to simulate the 2D infiltration processes for various soil textures and K_s, q, and θ_0 values. The soil hydraulic parameters and initial conditions are listed in Tables 2 and 4, respectively. Subsequently, the simulated values were compared with the estimated values obtained using the four models. The results are presented in Figure 4 and Table 6.

The results indicated that the proposed model exhibited the smallest estimation error in the horizontal and vertical wetting front advance, with MAE values of 4.27 and 6.20 cm, RMSE values of 6.20 and 6.58 cm, and MRE values of 5.61% and 7.15%, respectively. Following the proposed model, the AE model and the N model exhibited similar results. For horizontal and vertical wetting front advance, the AE model exhibited MAE values of 4.33 and 6.85 cm, RMSE values of 6.50 and 8.78 cm, and MRE values of 8.91% and 10.50%, respectively. For horizontal and vertical wetting front advance, N model exhibited MAE values of 5.12 and 4.88 cm, RMSE values of 6.44 and 6.74 cm, and MRE values of 9.50% and 8.55%, respectively. For horizontal and vertical wetting front advance, SZ model exhibited the largest error, with MAE values of 6.11 and 11.42 cm, RMSE values of 6.92 and 13.54 cm, and MRE values of 10.99% and 13.08%, respectively. Although the estimated values of the four models were close to the simulated ones, some differences were observed. The estimation model was based on measured or simulated values, and it helped simplify the complex infiltration process. The improved accuracy observed can be attributed to the initial soil water content, which was regarded as a variable in the estimation of the wetting front advance in the proposed model. Meanwhile, the proposed model was based on 12 soil textures (USDA soil texture classes), and can be estimated the soil wetting patterns of various soil textures, which is applicable to a variety of soil textures.

5. DISCUSSION

Overall, the model proposed in this study is more accurate than the other three models discussed (the SZ model, the N model, and the AE model) for estimating the wetting pattern in drip irrigation. This is mainly because the proposed model considers the effect of the initial soil water content on the wetting front advance, which is consistent with the actual situation. In addition, given the infiltration results obtained for 12 different soil textures (USDA soil texture classes), the model has a favorable level of universality.

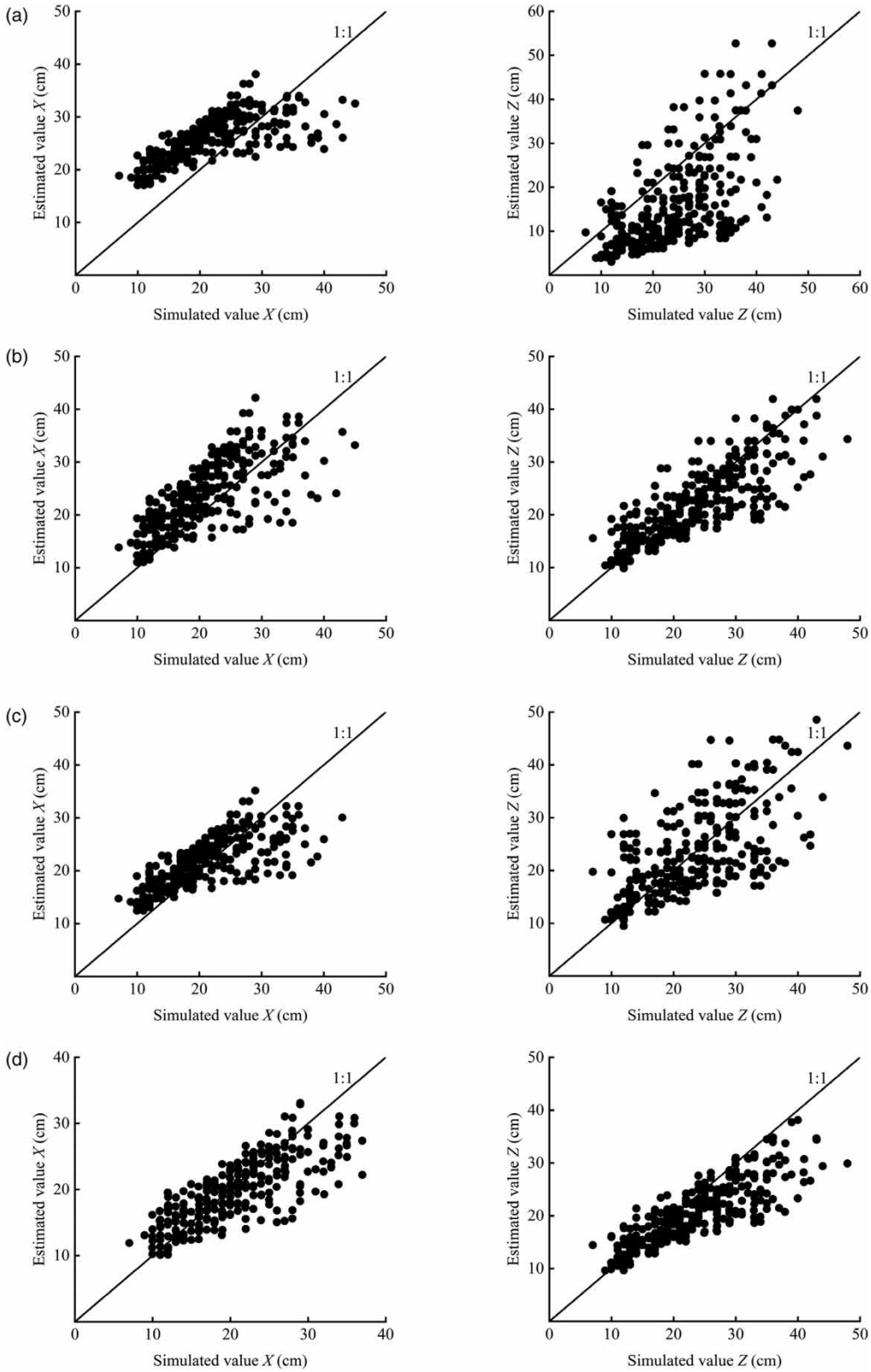

Figure 4 | Comparison of the simulated and estimated values of the horizontal X and vertical Z wetting front advance. (a) SZ model. (b) N model. (c) AE model. (d) Proposed model.

Table 6 | Error analysis of the simulated and estimated values of the wetting front advance

	Horizontal wetting front advance			Vertical wetting front advance		
	MAE (cm)	RMSE (cm)	MRE (%)	MAE (cm)	RMSE (cm)	MRE (%)
SZ model	6.11	6.92	10.99	11.42	13.54	13.08
N model	5.12	6.44	9.50	4.88	6.74	8.55
AE model	4.33	6.50	8.91	6.85	8.78	10.50
Proposed model	4.27	6.20	5.61	4.69	6.58	7.15

Note. MAE, mean absolute error; RMSE, root mean square error; MRE, mean relative error.

Soils with low water content have a small matrix potential (with negative values). The difference in potential energy increases the flow of water. Hence, the presence of low water content in the soil pores increases the time required to fill the pores with water, which in turn reduces the advance of the wetting front and increases the amount of water required (Liu *et al.* 2019; Patle *et al.* 2019; Cheng *et al.* 2021). When the water content increases, the difference in potential energy decreases, which decreases the flow of water, decreases the time required to fill the pores with water, accelerates the advance of the wetting front, and decreases the volume of applied water (Talsma 1974; Or *et al.* 2001; Guo & Liu 2019; Roy *et al.* 2020). This, however, contradicts the concept of dimensionless analysis, in which the advance of the wetting front is proportional to the total volume of applied water [Equation (4)]. This contradiction indicates that the initial soil water content has a major effect on soil water infiltration (Bauters *et al.* 2000). Therefore, the accuracy of the proposed model is higher than the AE model, the N model, and the SZ model (Figures 3 and 4, Tables 5 and 6).

Furthermore, the obtained results highlighted a large error in the estimation of the infiltration process of coarse-textured soils. As shown in Figure 5(a) and 5(b), compared with the measured values, the estimated horizontal and vertical wetting front advance of the proposed model without coarse-textured soils (sand, loamy sand, and sandy loam) demonstrated the following values: the MAE values were 2.77 and 2.41 cm, the RMSE values were 5.77 and 9.17 cm, and the MRE values were 9.06% and 7.60%, respectively. As shown in Figure 5(c) and 5(d), compared with the simulated values, for the horizontal and vertical wetting front advance, the MAE values were 4.12 and 3.78 cm, the RMSE values were 6.01 and 5.30 cm, and the MRE values were 6.46% and 4.75%, respectively. As shown in Tables 5 and 6, the MAE, RMSE, and MRE were reduced by 19.40%–32.20%, 13.57%–19.45%, and 21.02%–28.26%, respectively. These results indicated that the estimated results obtained without coarse-textured soils good agreed with the measured or simulated values. Compared with the estimation results obtained with coarse-textured soils, the error decreased (Figures 3(d) and 4(d)).

The results revealed relatively large errors in the estimation of the wetting front advance of coarse-textured soils, which is consistent with previous studies (Al-Ogaidi *et al.* 2016; Wang *et al.* 2020). The same results were also reflected in the SZ model, the N model, and the AE model for estimating wetting front advance in coarse-textured soils (not shown in this study). These results may be due to the presence of macropore flow during the infiltration of coarse-textured soils, a process that cannot be completely captured by Hydrus-2D/3D (Cameira *et al.* 2003; Jarvis *et al.* 2009). In addition to the matrix potential, the vertical wetting front advance is also affected by gravity potential. During the infiltration process, the water content and matrix potential of coarse-textured soils rapidly increase. When the water content reaches the field capacity, the soil water starts moving rapidly downward under the effect of gravity. Compared with soils of other textures (medium and fine soil textures), the vertical wetting front in coarse-textured soils advances much faster than the horizontal wetting front (Siyal & Skaggs 2009). Therefore, even for the same infiltration time and total volume of applied water, some errors may occur in the regression analysis of the vertical wetting front advance in coarse-textured soils, hence reducing the accuracy of the estimation model. To improve the accuracy of the soil wetting pattern model, the effect of the initial soil water content should be considered when estimating the wetting front advance. Therefore, the proposed model, with the initial soil water content considering simultaneously, provided a good estimation of the soil wetting pattern and was suitable for application in a variety of soil textures.

The proposed model is more accurate in estimating the soil wetting patterns without coarse-textured soils than coarse-textured soils. Further studies are required to deeply explore the mechanism of coarse-textured soil infiltration to improve the accuracy of the model when applied to a variety of soil textures. In recent research, many scholars (Kisi *et al.* 2021; Abdalrahman *et al.* 2022; Singh *et al.* 2022) have applied artificial intelligence (AI)-based approaches and data-driven

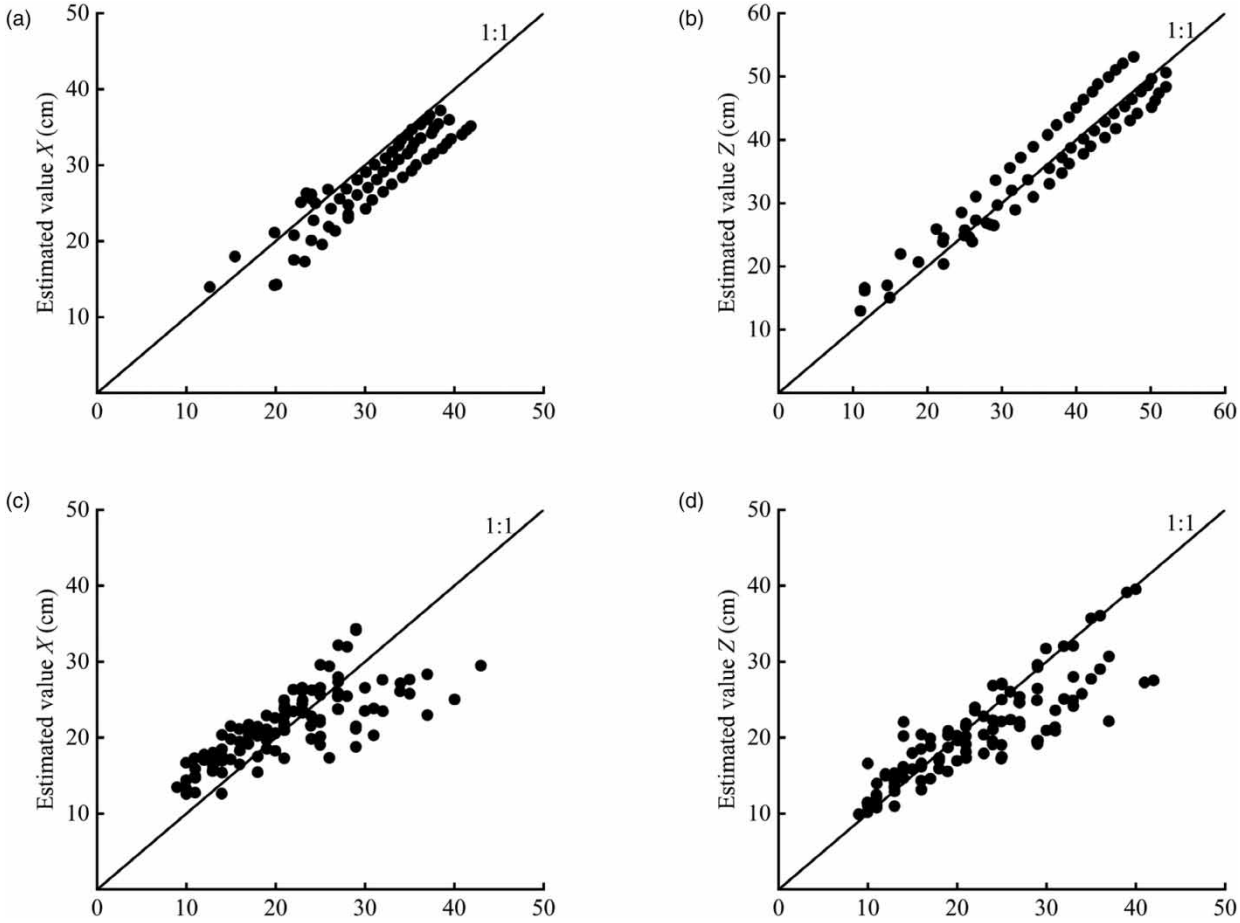

Figure 5 | Comparison of the measured/simulated and estimated values of wetting front advance without coarse-textured soils. (a) Measured value *X* (cm) (b) Measured value *Z* (cm) (c) Simulated value *X* (cm) (d) Simulated value *Z* (cm).

technologies (e.g., multi-layer perceptron (MLP), artificial neural network models (ANN), generalized regression neural network (GRNN), support vector machines (SVMs), and multivariate adaptive regression splines (MARS)) to irrigation system design and management. Therefore, a combination of these techniques and dimensional analysis theory should be considered in further studies to develop more applicable and accurate models of soil wetting patterns for drip irrigation.

6. CONCLUSION

In this study, we used the models proposed by Schwartzman & Zur (1986) and Naglič *et al.* (2014) as the basis for and added the initial soil water content to the proposed model of this study, which helped improve the estimation accuracy of the horizontal and vertical wetting front advance during drip irrigation. We then verified the reliability and universality of the proposed model by using experimental and simulated values in Hydrus-2D/3D. Compared with the SZ model, the N model, and the AE model, the proposed model of this study exhibited the smallest error in the horizontal and vertical wetting front advance distance, with MAE, RMSE, and MRE values ranging from 2.77 to 4.69 cm, from 6.20 to 10.61 cm, and from 5.61% to 10.51%, respectively. These results indicate that the proposed model is reliable and highly accurate and can be used with a variety of soil textures.

ACKNOWLEDGEMENTS

This research was supported by grants from the National Natural Science Foundation of China (52279043), and Scientific Research Program of the Shaanxi Provincial Education Department (20JS099).

DISCLOSURE STATEMENT

The authors declare that they have no conflict of interest.

DATA AVAILABILITY STATEMENT

All relevant data are included in the paper or its Supplementary Information.

CONFLICT OF INTEREST

The authors declare there is no conflict.

REFERENCES

Abdalrahman, G., Lai, S. H., Kumar, P., Ahmed, A. N., Sherif, M., Sefelnasr, A., Chau, K. W. & Elshafie, A. 2022 Modeling the infiltration rate of wastewater infiltration basins considering water quality parameters using different artificial neural network techniques. *Engineering Applications of Computational Fluid Mechanics* **16** (1), 397–421. https://doi.org/10.1080/19942060.2021.2019126.

Al-Ghobari, H. M. & Dewidar, A. Z. 2018 Integrating deficit irrigation into surface and subsurface drip irrigation as a strategy to save water in arid regions. *Agricultural Water Management* **209**, 55–61. https://doi.org/10.1016/j.agwat.2018.07.010.

Al-Ogaidi, A. A. M., Wayayok, A., Rowshon, M. K. & Abdullah, A. F. 2016 Wetting patterns estimation under drip irrigation systems using an enhanced empirical model. *Agricultural Water Management* **176**, 203–213. https://doi.org/10.1016/j.agwat.2016.06.002.

Amin, M. S. & Ekhmaj, A. I. 2006 DIPAC-drip irrigation water distribution pattern calculator. In *7th International Micro Irrigation Congress*, Vol. 1016.

Bauters, T. W. J., DiCarlo, D. A., Steenhuis, T. S. & Parlange, J. Y. 2000 Soil water content dependent wetting front characteristics in sands. *Journal of Hydrology* **231**, 244–254. https://doi.org/10.1016/S0022-1694(00)00198-0.

Brooks, R. H. & Corey, A. T. 1964 *Hydraulic Properties of Porous Media. Hydrology Paper No. 3*. Civil Engineering Department, Colorado State University, Fort Collins, Colorado, USA.

Buelow, M. C., Steenwerth, K. & Parikh, S. J. 2015 The effect of mineral-ion interactions on soil hydraulic conductivity. *Agricultural Water Management* **152**, 277–285. https://doi.org/10.1016/j.agwat.2015.01.015.

Cai, Y. H., Wu, P. T., Zhang, L., Zhu, D. L., Chen, J. Y., Wu, S. J. & Zhao, X. 2017 Simulation of soil water movement under subsurface irrigation with porous ceramic emitter. *Agricultural Water Management* **192**, 244–256. https://doi.org/10.1016/j.agwat.2017.07.004.

Cameira, M. R., Fernando, R. M. & Pereira, L. S. 2003 Soil macropore dynamics affected by tillage and irrigation for a silty loam alluvial soil in southern Portugal. *Soil and Tillage Research* **70** (2), 131–140. https://doi.org/10.1016/S0167-1987(02)00154-X.

Carsel, R. F. & Parrish, R. S. 1988 Developing joint probability distributions of soil water retention characteristics. *Water Resources Research* **24** (5), 755–769. https://doi.org/10.1029/WR024i005p00755.

Chai, T. & Draxler, R. R. 2014 Root mean square error (RMSE) or mean absolute error (MAE)? – Arguments against avoiding RMSE in the literature. *Geoscientific Model Development* **7** (3), 1247–1250. https://doi.org/10.5194/gmd-7-1247-2014.

Cheng, Q., Tang, C. S., Xu, D., Zeng, H. & Shi, B. 2021 Water infiltration in a cracked soil considering effect of drying-wetting cycles. *Journal of Hydrology* **593**, 125640. https://doi.org/10.1016/j.jhydrol.2020.125640.

Chu, X., Jia, X. & Liu, Y. 2018 Quantification of wetting front movement under the influence of surface topography. *Soil Research* **56** (4), 382–395. https://doi.org/10.1071/SR17071.

Cook, F. J., Thorburn, P. J., Fitch, P. & Bristow, K. L. 2003 Wetup: a software tool to display approximate wetting patterns from drippers. *Irrigation Science* **22** (3), 129–134. https://doi.org/10.1007/s00271-003-0078-2.

Cook, F. J., Fitch, P., Thorburn, P. J., Charlesworth, P. B. & Bristow, K. L. 2006 Modelling trickle irrigation: comparison of analytical and numerical models for estimation of wetting front position with time. *Environmental Modelling & Software* **21** (9), 1353–1359. https://doi.org/10.1016/j.envsoft.2005.04.018.

Cote, C. M., Bristow, K. L., Charlesworth, P. B., Cook, F. J. & Thorburn, P. J. 2003 Analysis of soil wetting and solute transport in subsurface trickle irrigation. *Irrigation Science* **22** (3), 143–156. https://doi.org/10.1007/s00271-003-0080-8.

Cristóbal-Muñoz, I., Prado-Hernández, J. V., Martínez-Ruiz, A., Pascual-Ramírez, F., Cristóbal-Acevedo, D. & Cristóbal-Muñoz, D. 2022 An improved empirical model for estimating the geometry of the soil wetting front with surface drip irrigation. *Water* **14** (11), 1827. https://doi.org/10.3390/w14111827.

Dai, Y., Shangguan, W., Duan, Q. Y., Liu, B. Y., Fu, S. H. & Niu, G. Y. 2013 Development of a China dataset of soil hydraulic parameters using pedotransfer functions for land surface modeling. *Journal of Hydrometeorology* **14** (3), 869–887. http://dx.doi.org/10.1175/JHM-D-12-0149.1.

Delgoda, D., Saleem, S. K., Malano, H. & Halgamuge, M. N. 2016 Root zone soil moisture prediction models based on system identification: formulation of the theory and validation using field and AQUACROP data. *Agricultural Water Management* **163**, 344–353. https://doi.org/10.1016/j.agwat.2015.08.011.

Fan, Y. W., Huang, N., Zhang, J. & Zhao, T. 2018 Simulation of soil wetting pattern of vertical moistube-irrigation. *Water* **10** (5), 601–620. https://doi.org/10.3390/w10050601.

Fan, Y. W., Yang, Z. W. & Wei, H. J. 2021 Establishment and verification of the prediction model of soil wetting pattern size in vertical moistube irrigation. *Water Supply* **21** (1), 331–343. https://doi.org/10.2166/ws.2020.326.

Green, W. H. & Ampt, G. A. 1911 Studies on soil physics, part I: the flow of air and water through soils. *Journal of Agricultural Science* **4**, 1–24.

Guo, K. & Liu, X. 2019 Effect of initial soil water content and bulk density on the infiltration and desalination of melting saline ice water in coastal saline soil. *European Journal of Soil Science* **70** (6), 1249–1266. https://doi.org/10.1111/ejss.12816.

Hill, D. E. & Parlange, J. Y. 1972 Wetting front instability in layered soils. *Soil Science Society of America Journal* **36** (5), 697–702. https://doi.org/10.2136/sssaj1972.03615995003600050010x.

Jarvis, N. J., Moeys, J., Hollis, J. M., Reichenberger, S., Lindahl, A. M. L. & Dubus, I. G. 2009 A conceptual model of soil susceptibility to macropore flow. *Vadose Zone Journal* **8** (4), 902–910. https://doi.org/10.2136/vzj2008.0137.

Jung, S. Y., Lim, S. & Lee, S. J. 2012 Investigation of water seepage through porous media using X-ray imaging technique. *Journal of Hydrology* **452**, 83–89. https://doi.org/10.1016/j.jhydrol.2012.05.034.

Kanda, E. K., Senzanje, A. & Mabhaudhi, T. 2020 Soil water dynamics under Moistube irrigation. *Physics and Chemistry of the Earth, Parts A/B/C* **115**, 102836. https://doi.org/10.1016/j.pce.2020.102836.

Kandelous, M. M. & Šimůnek, J. 2010 Comparison of numerical, analytical, and empirical models to estimate wetting patterns for surface and subsurface drip irrigation. *Irrigation Science* **28** (5), 435–444. https://doi.org/10.1007/s00271-009-0205-9.

Karimi, B., Mohammadi, P., Sanikhani, H., Salih, S. Q. & Yaseen, Z. M. 2020 Modeling wetted areas of moisture bulb for drip irrigation systems: an enhanced empirical model and artificial neural network. *Computers and Electronics in Agriculture* **178**, 1–13. https://doi.org/10.1016/j.compag.2020.105767.

Kilic, M. 2020 A new analytical method for estimating the 3D volumetric wetting pattern under drip irrigation system. *Agricultural Water Management* **228**, 105898. https://doi.org/10.1016/j.agwat.2019.105898.

Kisi, O., Khosravinia, P., Heddam, S., Karimi, B. & Karimi, N. 2021 Modeling wetting front redistribution of drip irrigation systems using a new machine learning method: adaptive neuro-fuzzy system improved by hybrid particle swarm optimization–Gravity search algorithm. *Agricultural Water Management* **256**, 107067. https://doi.org/10.1016/j.agwat.2021.107067.

Liu, Y., Cui, Z., Huang, Z., López-Vicente, M. & Wu, G. L. 2019 Influence of soil moisture and plant roots on the soil infiltration capacity at different stages in arid grasslands of China. *Catena* **182**, 104147. https://doi.org/10.1016/j.catena.2019.104147.

Moazenzadeh, R., Mohammadi, B., Safari, M. J. S. & Chau, K. W. 2022 Soil moisture estimation using novel bio-inspired soft computing approaches. *Engineering Applications of Computational Fluid Mechanics* **16** (1), 826–840. https://doi.org/10.1080/19942060.2022.2037467.

Molavi, A., Sadraddini, A., Nazemi, A. H. & Fard, A. F. 2014 Estimating wetting front coordinates under surface trickle irrigation. *Turkish Journal of Agriculture & Forestry* **36** (6), 729–737. https://doi.org/10.3906/tar-1202-74.

Moncef, H. & Khemaies, Z. 2016 An analytical approach to predict the moistened bulb volume beneath a surface point source. *Agricultural Water Management* **166**, 123–129. https://doi.org/10.1016/j.agwat.2015.12.020.

Moncef, H., Hedi, D., Jelloul, B. & Mohamed, M. 2002 Approach for predicting the wetting front depth beneath a surface point source: theory and numerical aspect. *Irrigation and Drainage: The Journal of the International Commission on Irrigation and Drainage* **51** (4), 347–360. https://doi.org/10.1002/ird.60.

Naglič, B., Kechavarzi, C., Coulon, F. & Pintar, M. 2014 Numerical investigation of the influence of texture, surface drip emitter discharge rate and initial soil moisture condition on wetting pattern size. *Irrigation Science* **32** (6), 421–436. https://doi.org/10.1007/s00271-014-0439-z.

Nie, W. B., Li, Y. B., Liu, Y. & Ma, X. Y. 2018 An approximate explicit Green–Ampt infiltration model for cumulative infiltration. *Soil Science Society of America Journal* **82** (4), 919–930. https://doi.org/10.2136/sssaj2017.11.0404.

Or, D., Wraith, J. M. & Warrick, A. W. 2001 Soil water content and water potential relationships. *Soil Physics Companion* **1**, 49–84. 10.1201/9781420041651.ch3.

Patle, G. T., Sikar, T. T., Rawat, K. S. & Singh, S. K. 2019 Estimation of infiltration rate from soil properties using regression model for cultivated land. *Geology Ecology & Landscapes* **3**, 1–13. https://doi.org/10.1080/24749508.2018.1481633.

Philip, J. R. 1984 Travel times from buried and surface infiltration point sources. *Water Resources Research* **20** (7), 990–994. https://doi.org/10.1029/WR020i007p00990.

Quirk, J. P. & Schofield, R. K. 1955 The effect of electrolyte concentration on soil permeability. *Journal of Soil Science* **6** (2), 163–178. https://doi.org/10.1111/j.1365-2389.1955.tb00841.x.

Revol, P., Clothier, B. E., Mailhol, J. C., Vachaud, G. & Vauclin, M. 1997 Infiltration from a surface point source and drip irrigation: 2. an approximate time-dependent solution for wet-front position. *Water Resources Research* **33** (8), 1869–1874. https://doi.org/10.1029/97WR01007.

Richards, L. A. 1931 Capillary conduction of liquids through porous mediums. *Physics* **1** (5), 318–333. https://doi.org/10.1063/1.1745010.

Rooij, G. H. D. 2000 Modeling fingered flow of water in soils owing to wetting front instability: a review. *Journal of Hydrology* **231**, 277–294. https://doi.org/10.1016/S0022-1694(00)00201-8.

Roth, R. L. 1974 Soil moisture distribution and wetting pattern from a point source. In *Proceedings of 2nd International Drip Irrigation Congress*, California, USA, pp. 246–251.

Roy, D., Jia, X., Steele, D. D., Chu, X. F. & Lin, Z. L. 2020 Infiltration into frozen silty clay loam soil with different soil water contents in the Red River of the North basin in the USA. *Water* **12** (2), 321. https://doi.org/10.3390/w12020321.

Schwartzman, M. & Zur, B. 1986 Emitter spacing and geometry of wetted soil volume. *Journal of Irrigation and Drainage Engineering* **112** (3), 242–253. https://doi.org/10.1061/(ASCE)0733-9437(1986)112:3(242).

Selim, T., Bouksila, F., Berndtsson, R. & Persson, M. 2013 Soil water and salinity distribution under different treatments of drip irrigation. *Soil Science Society of America Journal* **77** (4), 1144–1156. https://doi.org/10.2136/sssaj2012.0304.

Sharmasarkar, F. C., Sharmasarkar, S., Miller, S. D., Vance, G. F. & Zhang, R. 2001 Assessment of drip and flood irrigation on water and fertilizer use efficiencies for sugarbeets. *Agricultural Water Management* **46** (3), 241–251. https://doi.org/10.1016/S0378-3774(00)00090-1.

Shiri, J., Karimi, B., Karimi, N., Kazemi, M. H. & Karimi, S. 2020 Simulating wetting front dimensions of drip irrigation systems: multi criteria assessment of soft computing models. *Journal of Hydrology* **585**, 124792. https://doi.org/10.1016/j.jhydrol.2020.124792.

Šimůnek, J., Van Genuchten, M. T. & Šejna, M. 2006 The HYDRUS software package for simulating two-and three-dimensional movement of water, heat, and multiple solutes in variably-saturated media. *Technical Manual, Version* **1**, 241.

Singh, V. K., Panda, K. C., Sagar, A., Al-Ansari, N., Duan, H. F., Paramaguru, P. K., Vishwakarma, D. K., Kumar, A., Kumar, D., Kashyap, P. S., Singh, R. M. & Elbeltagi, A. 2022 Novel genetic algorithm (GA) based hybrid machine learning-pedotransfer function (ML-PTF) for prediction of spatial pattern of saturated hydraulic conductivity. *Engineering Applications of Computational Fluid Mechanics* **16** (1), 1082–1099. https://doi.org/10.1080/19942060.2022.2071994.

Siyal, A. A. & Skaggs, T. H. 2009 Measured and simulated soil wetting patterns under porous clay pipe sub-surface irrigation. *Agricultural Water Management* **96** (6), 893–904. https://doi.org/10.1016/j.agwat.2008.11.013.

Skaggs, T. H., Trout, T. J., Šimůnek, J. & Shouse, P. J. 2004 Comparison of HYDRUS-2D simulations of drip irrigation with experimental observations. *Journal of Irrigation and Drainage Engineering* **130** (4), 304–310. 10.1061/(ASCE)0733-9437(2004)130:4(304).

Skaggs, T. H., Trout, T. J. & Rothfuss, Y. 2010 Drip irrigation water distribution patterns: effects of emitter rate, pulsing, and antecedent water. *Soil Science Society of America Journal* **74** (6), 1886–1896. https://doi.org/10.2136/sssaj2009.0341.

Sreelash, K., Buis, S., Sekhar, M., Ruiz, L., Tomer, S. K. & Guerif, M. 2017 Estimation of available water capacity components of two-layered soils using crop model inversion: effect of crop type and water regime. *Journal of Hydrology* **546**, 166–178. https://doi.org/10.1016/j.jhydrol.2016.12.049.

Subbaiah, R. 2013 A review of models for predicting soil water dynamics during trickle irrigation. *Irrigation Science* **31** (3), 225–258. https://doi.org/10.1007/s00271-011-0309-x.

Surendran, U. & Chandran, K. M. 2022 Development and evaluation of drip irrigation and fertigation scheduling to improve water productivity and sustainable crop production using HYDRUS. *Agricultural Water Management* **269**, 107668. https://doi.org/10.1016/j.agwat.2022.107668.

Talsma, T. 1974 The effect of initial moisture content and infiltration quantity on redistribution of soil water. *Australian Journal of Soil Research* **12** (1), 15–26. https://doi.org/10.1071/SR9740015.

Van Genuchten, M. T. 1980 A closed-form equation for predicting the hydraulic conductivity of unsaturated soils. *Soil Science Society of America Journal* **44** (5), 892–898. https://doi.org/10.2136/sssaj1980.03615995004400050002x.

Vishwakarma, D. K., Kumar, R., Kumar, A., Kushwaha, N. L., Kushwaha, K. S. & Elbeltagi, A. 2022 Evaluation and development of empirical models for wetted soil fronts under drip irrigation in high-density apple crop from a point source. *Irrigation Science* 1–24. https://doi.org/10.1016/j.rser.2019.01.040.

Wang, F. X., Kang, Y. & Liu, S. P. 2006 Effects of drip irrigation frequency on soil wetting pattern and potato growth in North China Plain. *Agricultural Water Management* **79** (3), 248–264. https://doi.org/10.1016/j.agwat.2005.02.016.

Wang, C., Bai, D., Li, Y. B., Wang, X. D., Pei, Z. & Dong, Z. C. 2020 Infiltration characteristics and spatiotemporal distribution of soil moisture in layered soil under vertical tube irrigation. *Water* **12** (10), 2725. https://doi.org/10.3390/w12102725.

Willmott, C. J., Robeson, S. M. & Matsuura, K. 2012 A refined index of model performance. *International Journal of Climatology* **32** (13), 2088–2094. https://doi.org/10.1002/joc.2419.

Witelski, T. P. 2005 Motion of wetting fronts moving into partially pre-wet soil. *Advances in Water Resources* **28** (10), 1133–1141. https://doi.org/10.1016/j.advwatres.2004.06.006.

Yang, W. H., Clifford, D. & Minasny, B. 2015 Mapping soil water retention curves via spatial Bayesian hierarchical models. *Journal of Hydrology* **524**, 768–779. https://doi.org/10.1016/j.jhydrol.2015.03.029.

Yu, C. & Zheng, C. M. 2010 HYDRUS: software for flow and transport modeling in variably saturated media. *Groundwater* **48** (6), 787–791. https://doi.org/10.1111/j.1745-6584.2010.00751.x.

First received 3 August 2022; accepted in revised form 8 December 2022. Available online 19 December 2022